

CALCULATING POTENTIAL AND ACTUAL EVAPORATION FROM A BARE SOIL SURFACE BY SIMULATION OF CONCURRENT FLOW OF WATER AND HEAT¹

C. H. M. van BAVEL and D. I. HILLEL*

Department of Soil and Crop Sciences, Texas Agricultural Experiment Station, Texas A and M University, College Station, Texas, 77843 (U.S.A.)

(Received August 2, 1976; accepted September 30, 1976)

ABSTRACT

Van Bavel, C. H. M. and Hillel, D. I., 1976. Calculating potential and actual evaporation from a bare soil surface by simulation of concurrent flow of water and heat. *Agric. Meteorol.* 17: 453–476.

A numerical method is described by which the instantaneous evaporation rate from bare soil, regardless of its wetness, can be estimated from standard weather data and the physical characteristics of the soil profile. It is used to calculate potential evaporation from a surface energy balance without the commonly used approximations. The results show that the soil heat flux and the soil surface emittance may vary enough with soil water content so as to make the concept of potential evaporation ambiguous. From a practical viewpoint, however, these differences in the evaporation rate from a wet surface are not large enough to invalidate the simpler combination or energy balance formulas, in which the surface albedo and roughness are the only non-climatic parameters.

The method is particularly useful in simulating the evaporation process from drying surfaces. The results support the existence of separate potential and falling rate stages of evaporation, but not that of a third, constant rate stage. A rapid increase of the diurnal amplitude of the surface temperature is the clearest indicator of the transition between the two stages.

INTRODUCTION

Potential evaporation (E_p) is generally conceived as the water vapor flux density ($\text{kg m}^{-2} \text{s}^{-1}$, or mm s^{-1}) from a surface that is externally wet, so that, at the surface boundary, the air is at saturation humidity. Therefore, the actual evaporation (E_a) cannot exceed the potential value. It will be less if the relative humidity at the evaporating surface is less than unity.

It is of practical importance to be able to calculate E_p from commonly available weather data. The combination method, first used by Penman

* On leave from Department of Soil and Water Science, The Hebrew University of Jerusalem, Rehovot, Israel.

(1948), is a standard approach to the problem. Its essential objective was to avoid the need to know the surface temperature. Thus, in the original Penman version the surface temperature was assumed to be equal to the air temperature in estimating the longwave radiance of the surface and the slope of the temperature vs. saturation humidity relation.

Though the combination method purports to rely on standard weather data only, it also requires knowledge of properties of processes related to the surface and the underlying soil profile, including the surface albedo and emittance, the surface radiance as a function of its temperature, the surface roughness, and the soil heat flux. The stability of the air in the boundary layer must also be considered, since it influences the turbulent transfer of heat and vapor in the air.

Of all the parameters listed, Penman (1948) took account only of the surface albedo. His result was therefore restricted in validity to periods of several days, and to a standard (open water) surface. To broaden the scope of the method, Van Bavel (1966) proposed to use actually measured values of net radiation and soil heat flux, and to account for the surface roughness. He found that when so modified, the method gave valid results for periods as short as one hour, for both open water and bare, wet soil. This result is not however, necessarily applicable to all situations; moreover, it requires knowledge of two parameters, net radiation and soil heat flux, that are not in the category of commonly available data.

In this report we propose a comprehensive method that accounts for all major factors involved in determining the evaporative flux, and that requires only the following common weather variables: global, shortwave irradiance, air temperature, air humidity, and wind speed. It remains a combination method, in that the surface energy balance is combined with the simultaneous transport of heat and water vapor in the air above the surface, as well as the simultaneous transport of heat and liquid water in the soil below the surface.

We will develop the method for the simple case of a bare soil surface, and a soil of homogeneous hydraulic and thermal properties. We will show that the result is not only capable of giving the potential evaporation, but also the actual evaporation for periods when the soil surface is dry. Thus, the method encompasses the entire process of the drying of an initially wet soil, conventionally described as consisting of separate "stages" (see for example, Hillel, 1971). At present there is no universal theory that predicts the progressive drying of a soil surface.

METHOD

The general method employed is that of dynamic numerical simulation. This means that, starting with specified initial conditions, the properties and processes in the soil-atmosphere system are repeatedly updated, using as the inputs only the time-dependent weather variables: global irradiance (R_g , W m^{-2}), air temperature (T_a , $^{\circ}\text{C}$), air dewpoint (T_d , $^{\circ}\text{C}$), and windspeed (S_a , m s^{-1}), the

last three at standard height (2.0 m).

The calculations are done by a program written in S360/CSMP, a specific simulation language suitable for time-variant systems, though other computer languages could be employed as well. The general principles of this method were set forth by De Wit and Van Keulen (1972). A provisional approach to the present problem was outlined by Van Bavel and Hillel (1975) and a solution similar in concept to the present one was given by Van Keulen (1975).

Weather parameters

Hourly values for the four input parameters were extracted from standard U.S. Weather Service records as long-time averages for the month of June, obtained at 7 different locations in the U.S. Windspeeds, generally measured at elevations other than 2 m, were corrected for the difference. The standard records give only the 24 h totals of R_g , conventionally called "solar radiation", but herein termed global irradiance. It was assumed that these totals would be distributed over the daylight period in proportion to the sine of the sunangle, and a separate calculation was made for each location to obtain the hourly values. Variable cloudiness during the day was not accounted for.

For the Lubbock location, Texas, a set of data was used, in addition to the "mean" set, to represent a day of unusually high evaporative demand. These data were typified by a totally clear sky and high windspeeds, as seen in Table I.

In the CSMP program the climatic data are entered as tables of hourly values, and the program interpolates linearly in between for each updating calculation. The general climatic characteristics of each location are given in Table I. They cover a range from the temperate and humid climate of Seattle to the desert conditions of Phoenix, and pertain to a time of year at which evaporative demand is at or near its peak.

As the simulation is continuous, starting from a suitably chosen initial condition, it may have to proceed for several days to give the desired condition. For that purpose the daily pattern of weather variables was assumed to be repetitive. In reality, a constant succession of "average June" days will never occur in the same way, but the procedure should, nevertheless, give results representative for each location.

Surface energy balance

At the soil surface the following is stipulated:

$$R_n + LE + A + S = 0 \quad (1)$$

All components of the energy balance are referred to the surface, so that, in the daytime, net irradiance (R_n , $W m^{-2}$) is positive, the product of the latent

TABLE I

Elevation (E_1), average daily total of global irradiance (R_g), average daily temperature (T_a), dewpoint (T_d), and windspeed at 2 m (S_a), for the month of June at 7 different first-order stations; also extreme data for global irradiance and windspeed at Lubbock, Texas.

	E_1 (m)	R_g (MJ m ⁻²)	T_a (°C)	T'_d (°C)	S_a (m s ⁻¹)
Binghamton, N.Y.	499		18.0	13.9	1.45
Ithaca, N.Y.*		20.65			
De Moines, Iowa	294		21.7	16.4	1.69
Ames, Iowa*		21.63			
Houston, Texas	33		26.5	24.3	1.20
Lake Charles, La.*		23.31			
Lubbock, Texas	988		25.2	15.9	2.09
Midland, Texas*		26.33			
Lubbock, Texas**	988		25.2	15.9	4.50
Midland, Texas**		30.34			
Phoenix, Ariz.	337	28.14	29.6	8.1	1.30
Sacramento, Calif.	8		21.9	14.3	1.25
Davis, Calif.*		28.78			
Seattle-Tacoma, Wash.	137	22.09	15.4	12.3	1.58

*For global irradiance data the closest nearby station was used whenever indicated.

**Extreme data.

heat of water (L , J kg⁻¹) and the evaporation rate (E , kg m⁻² s⁻¹) is negative, the sensible heat flux to the air (A , W m⁻²) generally negative, and the soil sensible heat flux (S , W m⁻²) generally negative. The flux of sensible heat in the soil associated with liquid flux of soil water is ignored as negligible as is any net evaporation below the surface and the associated water vapor flux in the soil. However, the latent heat flux caused by intermittent evaporation and condensation, as originally described by De Vries (1966), is taken into account, as we will describe later.

The value of R_n is found as:

$$R_n = (1 - a)R_g + R_1 - \epsilon \sigma (T_s + 273.16)^4 \quad (2)$$

In eq.2, R_1 (W m⁻²) is the longwave sky irradiance and T_s the surface temperature (°C). The albedo (a) is not a constant, but is made dependent upon the wetness of the superficial layer of soil (w_1 , m³ m⁻³) in a simple, linear fashion:

$$\begin{aligned} w_1 > 0.25 & \quad a = 0.10 \\ w_1 < 0.10 & \quad a = 0.25 \\ 0.10 < w_1 < 0.25 & \quad a = 0.10 + (0.25 - w_1) \end{aligned} \quad (3)$$

The numbers used in eq.3 are mean values abstracted from the literature, such as Sellers (1965) and Linacre (1969), and from a consideration of the water

retention of the soil chosen for the simulation.

The longwave radiation (R_l , $W m^{-2}$) from the sky is calculated, as was done by Penman (1948), from Brunt's formula in the form given by Sellers (1965):

$$R_l = \sigma(T_a + 273.16)^4 (0.605 + 0.048 \sqrt{1370 H_a}) \quad (4)$$

In eq.4, H_a is the air humidity ($kg m^{-3}$), calculated from the dewpoint, T_d , which is an input.

Finally, in the third term of eq.2, T_s is the surface temperature, and ϵ the surface emittance. Similar to the value of a , ϵ is dependent upon w_1 , as follows:

$$\epsilon = 0.90 + 0.18 w_1 \quad (5)$$

This provides that, for a totally dry surface, the value of ϵ is 0.90 and for a saturated soil, i.e. $w_1 = 0.45$, $\epsilon = 0.98$. The numerical values used are adapted from measurements reported by Sellers (1965) and by Conway and Van Bavel (1967).

It should be clear from eq.2 e.f. that the value of R_n , and thus the entire energy balance, depends in part upon transient surface properties (a and ϵ), as well as the unknown value of T_s .

The remaining terms in eq.1 will be developed in the following sections as they represent transport processes in the air and in the soil.

Transport of sensible heat and water vapor in the air

The values of A and E in eq.1 are found in the conventional manner by defining, first, the reciprocal of the turbulent transport coefficient between the surface and the reference elevation (2 m) as the aerodynamic resistance, R_c ($s m^{-1}$) as follows:

$$R_c = R_a \cdot St \quad (6)$$

R_a is the adiabatic or neutral value of R_c , and St the stability correction. This parameter can be defined after Szeicz et al. (1973), following Monteith (1963), as:

$$St = 1/(1 - 10Ri) \quad (7)$$

and Ri , the Richardson number, as:

$$Ri = 9.81 (2 - Z_0) (T_a - T_s) / [(T_a + 273.16) S_a^2] \quad (8)$$

The surface roughness Z_0 (m) enters into the correction, as well as the unknown surface temperature T_s , and the windspeed, S_a . Further:

$$R_a = [\ln (2.0/Z_0)]^2 / 0.16 S_a \quad (9)$$

There is a voluminous literature of alternative and more detailed methods for calculating R_c or its equivalent (see, for example Pruitt et al., 1973). We have chosen a simple approach which is widely used. Finally we define:

$$A = (T_a - T_s) C/R_c \quad (10)$$

and:

$$E = (H_s - H_a)/R_c \quad (11)$$

$C(\text{J m}^{-3})$ is the volumetric specific heat of air and H_s (kg m^{-3}) the absolute humidity of the air at the soil surface.

At this point we introduce an important consideration by specifying that H_s depends not only upon the surface temperature, but also the surface water content. If H_0 is the saturation humidity at the surface temperature, w_1 the wetness of the surface layer, and p_1 (m water column) the pressure potential associated with this value, we utilize the standard thermodynamic equivalence:

$$H_s = H_0 \exp [p_1/46.97 (T_s + 273.16)] \quad (12)$$

Note that p_1 always has a negative value, so that, for example, if $p_1 = -100$ m, then the relative humidity (H_s/H_0), at $T_s = 30^\circ\text{C}$ equals 0.993.

This approach is approximate in that it assumes that the water content of the surface layer (0.01 m) is equal to that of the very surface. However, it is more general than the empirical relations, such as used by Ritchie (1972), or by Hillel et al. (1975), for example.

The relation between soil wetness and pressure potential is specified by a table, as discussed further on.

Transport of sensible heat and water in the soil

The energy balance equation (eq.1) leaves one term unspecified to this point, the soil heat flux S , which is found from:

$$S = 2(T_1 - T_s) K_1/D_1 \quad (13)$$

in which T_1 is the temperature at the center of the surface layer, K_1 ($\text{W m}^{-1} \text{s}^{-1}$) its thermal conductivity, and D_1 (m) its thickness.

For the surface layer of soil we can also write:

$$D_1(d(w_1)/dt) = E - C_{1,2}(h_2 - h_1) (D_1 + D_2)/2 \quad (14)$$

That is, the time rate of change of the water content of the top layer must equal the flux at the surface E diminished by the flux of water across the bottom, which is found from Darcy's Law. In this case, the bottom flux is found from the average hydraulic conductivity of soil layers 1 and 2 ($C_{1,2}$), and the gradient of the hydraulic potential (h), as shown in eq.14. Since E is negative and generally greater than the bottom flux, which is usually also negative (upward), the value of $d(w_1)/dt$ is, generally negative, indicating a decrease in water content. When E is small, as at night, eq.14 can give positive values, or a rewetting of the surface layer.

Eqs.13 and 14 connect the surface fluxes of heat and water with those in

the soil. There they obey the usual flow equations, and the requirements of conservation of mass and energy. To make practical use of Eqs.13 and 14 the changing conditions in the entire body of soil, however defined, must be accounted for. In this we use a method described in general terms by De Wit and Van Keulen (1972), and as used for the isothermal flow of water, by, for example, Van Bavel et al. (1973), Hillel et al. (1975), or for the flow of heat by Wierenga and De Wit (1970). We can combine the flow of both heat and water without complications, as long as it is specified that the two processes are independent, as stated above. A much more detailed method for calculating water and heat flows would follow from the theory of Philip and De Vries (1957), as recently exemplified by Jackson et al. (1974), who, however, did not predict the heat flows, nor the soil temperatures as we do in the present approach.

The soil was typified by its hydraulic characteristics, representative of a loam soil, as shown in Fig.1. These relations, introduced into the program as tables, enable the program to find, at each updating time, the pressure potential and the hydraulic conductivity pertaining to the water content, layer by layer. The thermal properties of the soil were also specified, following the methods given by De Vries (1966). Thus, at each updating, the heat capacity and the thermal conductivity are found from the fixed material properties and the changing soil water content and temperature, again layer by layer.

As a representative case, we postulated a total soil depth of 1.13 m, assuming that the soil heat flux at that depth would be zero and that the water flux would equal the hydraulic conductivity of the last layer, equivalent to the assumption of a unit hydraulic gradient or zero wetness gradient. The soil was divided into 14 layers of increasing thickness starting with a 0.01 m surface layer. Its total porosity was 0.45 and its saturated conductivity $0.5 \cdot 10^{-5} \text{ m s}^{-1}$, or 432 mm day⁻¹.

General aspects of simulation method

The difference between calculating the potential evaporation rate by dynamic simulation, as described above, and the historical approach to date is that the latter is based upon the arbitrary assumption that the properties of the soil, including the surface, but excepting its temperature, are static, regardless of the changing meteorological input or the evaporation process itself, and that the transport process in the atmosphere is likewise unaffected. The present approach is more comprehensive so as to be more realistic, but it does require specification of the initial condition. For this we chose a saturated condition of the entire profile, i.e., a wetness of 0.45 and a soil temperature distribution with depth equal to that of the average daily temperature on June 15, if the soil were at a constant wetness of 0.15. The simulation was always started at midnight, allowing some time for profile equilibration prior to the onset of evaporation in the morning.

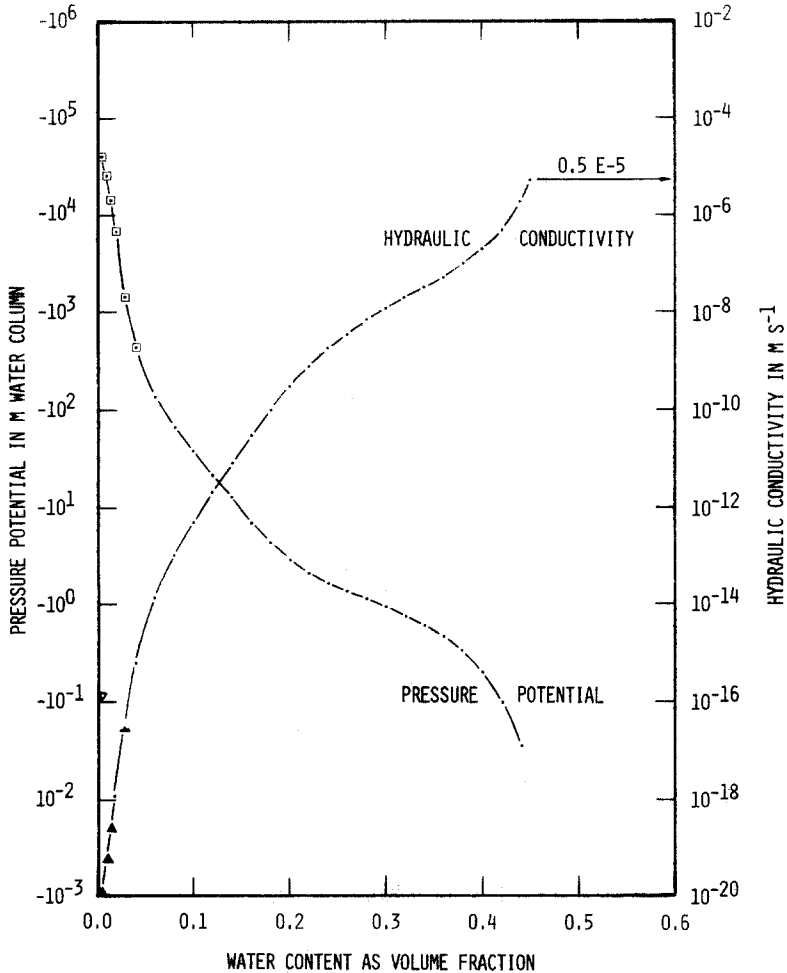


Fig.1. Hydraulic conductivity and pressure potential as a function of water content for a loam soil. The saturation water content is 0.45 and the corresponding conductivity is $0.5 \cdot 10^{-5} \text{ m s}^{-1}$.

A 3 day-run was made for all data sets described in Table I to find the potential evaporation pattern. A 10-day run was made for Lubbock to demonstrate the transition from potential evaporation to actual evaporation at considerably reduced rates, and 20-day runs for Phoenix and Binghamton to explore the contrast between two extreme climate types.

The computing method is the same as in previously described uses of CSMP. A variable timestep updating method is used so as to keep the changes in the updated quantities below 0.10% in each update. One point requires emphasis. Whereas the updating of the soil wetness and the soil temperature is simple and explicit, the surface temperature cannot be so simply determined. Its value appears simultaneously and implicitly in eqs.1, 2, 8, 10, 11,

12, and 13. These constitute a system of 7 equations with 7 unknowns (R_n , E , A , S , T_s , Ri , and H_o), of which only T_s cannot be stated explicitly. Thus, a special CSMP function, IMPL, is used to find the proper value of T_s at each update, by an iterative method.

A problem exists with eq.7. Obviously, if Ri should equal +0.1 or be greater, an absurd result would be obtained. This condition would be indicative of an extreme inversion, at very low windspeed, as eq.8 indicates. To prevent this incidence, the value of Ri was limited at +0.08.

RESULTS AND DISCUSSION

Potential evaporation

The calculations made for a consecutive 10 days drying period using the Lubbock weather data showed that, during the first four days, the relative humidity at the soil surface was always 100%. On the fifth day in the afternoon the surface layer became so dry that the relative humidity fell to 88% for a short period after which it rose again.

Thus, during the first four days the traditional condition for potential evaporation was met. However, this did not result in equal values for the evaporation rate, nor for the other components of the surface energy balance, as shown in Table II. From the first day on, the 24-h evaporation rates declined from 8.02 mm to 7.02 mm on the fourth day, or by 12% of its original value. This is significant and shows that the traditional concept of potential evaporation is not precise.

The causes of the decline in evaporation rate shown in Table II are several and they are not simply related. Obviously, the emittance and longwave radiance decline with time as the initially saturated profile loses water by drainage and by drying of the surface. But, beginning with the third day, the albedo rises and less shortwave energy is retained. Further, as the soil drains and dries, its thermal conductivity and its heat capacity decrease, affecting the soil heat flux. Results, not shown in Table II, suggest that the surface temperature and the air stability have the same diurnal pattern on each of the first four days, and are therefore not related to the change in evaporation rate.

The net result of the physical changes in the soil profile, exposed to identical weather conditions, is that the net radiant flux decreases significantly with time, as does the soil heat flux, both shown in Table II.

The second day represents a condition where an initially saturated profile had drained freely for at least 24 h. This condition, often referred to as "field capacity", is by no means a final one as the daily drainage figures in Table II show. However, to give a better definition of potential evaporation, we might suggest, albeit arbitrarily, that it be taken as the evaporation rate that prevails on the second day following an initial condition of saturation of the soil profile, provided the condition of a 100% relative humidity at the

TABLE II

Processes and properties at the surface of a loam profile, initially saturated, exposed to average June weather conditions at Lubbock, Texas

Day	Evaporation (mm)	Drainage (mm)	Net radiation (MJ m^{-2})	Soil heat flux (MJ m^{-2})	Emittance at noon	Albedo at noon	Wetness*
1	8.02	66.9	17.32	2.15	.960	0.100	0.318
2	7.69	15.6	17.53	1.03	.948	0.100	0.250
3	7.38	10.2	16.84	0.91	.936	0.147	0.193
4	7.02	7.7	15.91	0.84	.912	0.208	0.124

*Of surface layer at end of day.

surface is always met. Accordingly, defining potential evaporation from a very coarse textured soil may actually not be feasible. Nevertheless, the proposed definition may well be sufficiently precise for practical purposes.

The dynamic nature of the evaporating system is further portrayed by Fig.2, which gives the hourly values of emittance, albedo and soil heat flux during the first four days of drainage and drying. Note the evident rewetting of the surface layers during the night, implying that during much of the period there is upward movement (rise) of liquid water toward the surface and, simultaneously, downward movement (drainage) in the lower part of

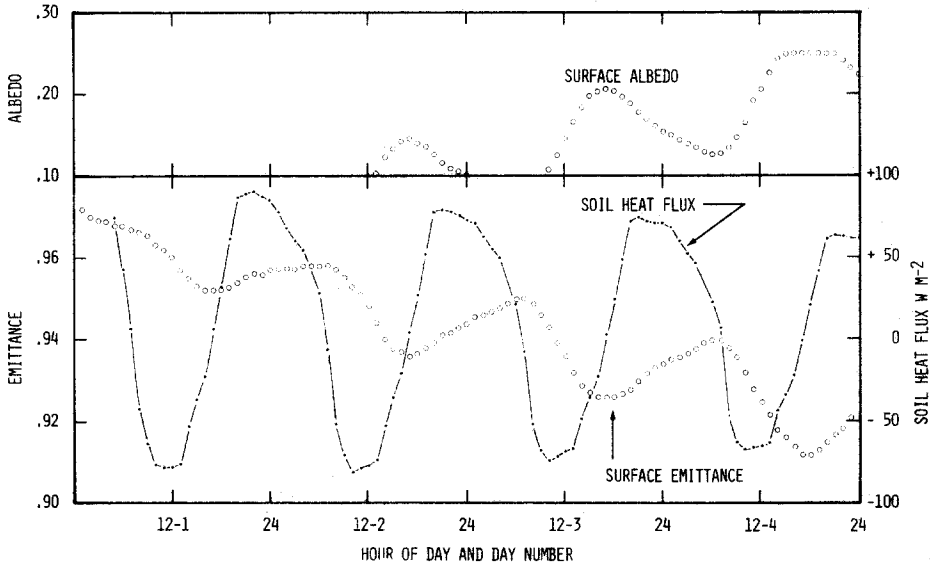


Fig.2. Hourly values of surface albedo (top) and of surface emittance and soil heat flux (bottom) of a loam soil profile that, saturated at time 0, is allowed to drain freely and to evaporate in an environment typified by average hourly weather parameters for June in Lubbock, Texas. During the entire period the surface relative humidity is 1.0.

the profile (see also Hillel, 1975).

Based on the foregoing analysis, a comparison of our model calculations between different summer weather conditions in the U.S. was confined to the numbers calculated for the second day after initial saturation of the loam profile. These results are given in Table III.

The June values for the potential evaporation range from 4.5 mm per day in the temperate climate of Binghamton to 8.1 mm per day in Phoenix. In appraising these results, shown in Table III, it should be remembered that they are calculated from average weather data and that, on any given day, the evaporation rates may be either lower or higher. As an example, by using data for Lubbock, Texas that typify a clear and windy day, we calculated an evaporation rate of 12.1 mm per day.

The day totals for the energy balance, also shown in Table III, reveal that in a temperate and humid environment the evaporation energy flux is less than the net radiant balance (R_n), and that the reverse is true in arid locations. This phenomenon, known as advection, is more precisely characterized by the day total of A , the sensible heat transport in the air. In the humid environment it is a negative quantity, indicating a net heating of the air, whereas in an arid location it is positive. On a windy day this effect is much enhanced, as the second entry for Lubbock in Table III shows.

In all cases a wet soil profile loses heat, as all values for S in Table III are

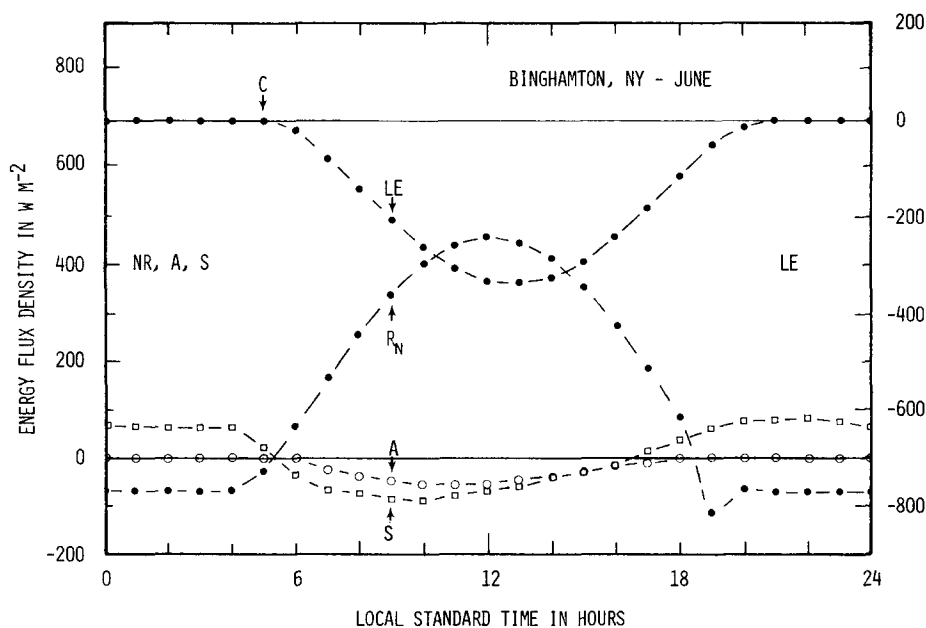


Fig. 3. Typical energy-balance partition prevailing during potential evaporation in a temperate humid summer climate from a loam soil profile. Shown are net radiant flux (R_n), latent heat flux (LE), sensible heat flux into the air (A), and into the soil (S). A positive sign indicates a flux toward the surface and C marks the incidence of condensation.

TABLE III

Daily totals of evaporation (E), drainage (D), global irradiance (R_g), the components of the surface energy balance, the maximum and minimum surface temperature ($T_{s, \max}$ and $T_{s, \min}$), and the surface temperature amplitude (Ampl) for 7 locations on the second day after drainage from a saturated profile has commenced

Location	E (mm)	D (mm)	R_g (MJ m ⁻²)	R_n (MJ m ⁻²)	LE (MJ m ⁻²)	A (MJ m ⁻²)	S (MJ m ⁻²)	$T_{s, \max}$ (°C)	$T_{s, \min}$ (°C)	Ampl. (°C)
Binghamton, N.Y.	4.55	15.69	20.65	+11.82	-11.11	-1.39	+0.68	24.0	12.8	11.2
Seattle, Wash.	4.63	15.71	22.09	+12.82	-11.31	-2.05	+ .74	21.9	11.0	10.9
Des Moines, Iowa	5.35	15.64	21.63	+13.23	-13.06	-0.81	+ .65	27.0	15.9	11.1
Houston, Texas	6.06	15.62	23.31	+15.53	-14.81	-1.80	+1.08	32.5	23.1	9.4
Sacramento, Calif.	7.70	15.51	27.78	+18.73	-18.78	-0.87	+1.00	31.0	14.1	16.9
Lubbock, Texas	7.69	15.56	26.33	+17.53	-18.78	+0.20	+1.03	30.2	18.1	12.1
Phoenix, Ariz.	8.06	15.47	28.14	+17.36	-19.69	+0.51	+1.82	34.8	18.9	15.9
Lubbock, Texas*	12.07	15.32	30.34	+20.56	-29.48	+7.94	+1.98	26.2	16.8	9.4

*Extreme June weather data.

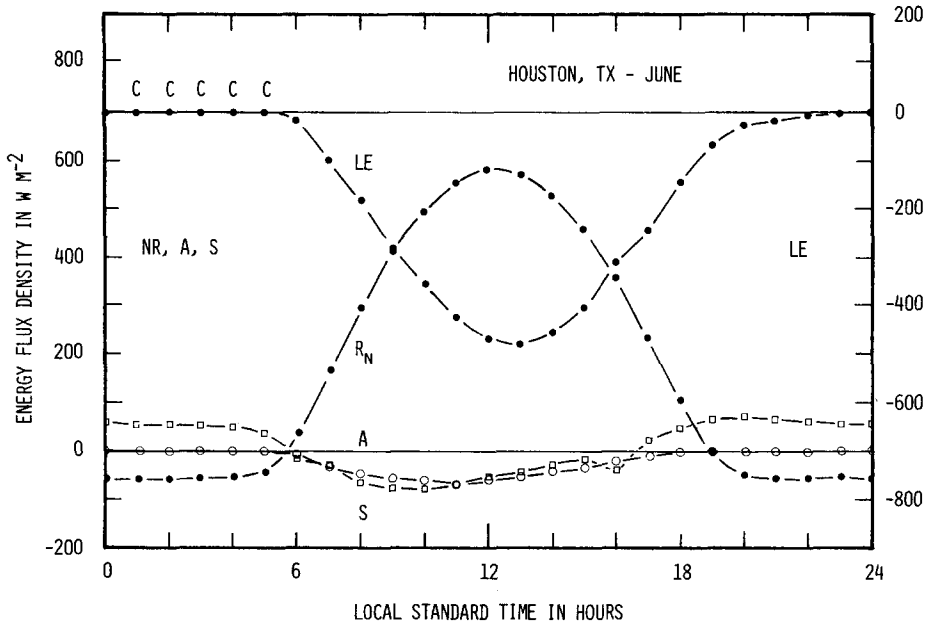


Fig. 4. Typical energy-balance partition prevailing during potential evaporation in a hot and humid summer climate from a loam soil profile. Shown are net radiant flux (R_N), latent heat flux (LE), sensible heat flux into the air (A), and into the soil (S). A positive sign indicates a flux toward the surface and C marks the incidence of condensation.

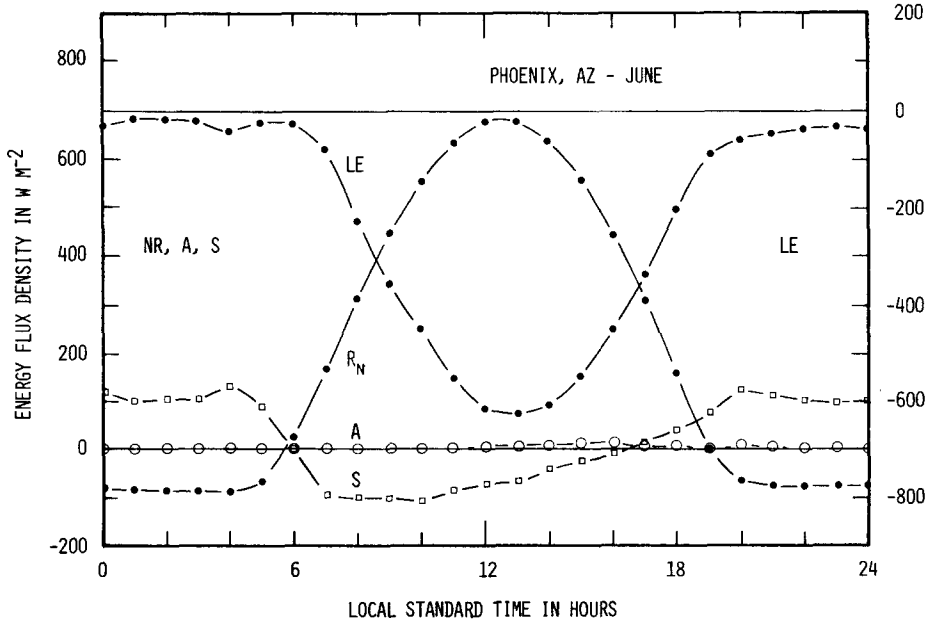


Fig. 5. Typical energy-balance partition prevailing during potential evaporation in a hot and dry summer climate from a loam soil profile. Shown are net radiant flux (R_N), latent heat flux (LE), sensible heat flux into the air (A), and into the soil (S). A positive sign indicates a flux toward the surface and C marks the incidence of condensation.

positive and, again, the value of S is much larger in an arid environment. We can also conclude that neglecting the soil heat flux in the combination method may cause an error in the energy balance of bare soil of between 5% and 10% and result in underestimation of E . When evaporative demand is higher than average, the error will be larger.

The calculated values of the surface temperature show that, as expected, the climate of a wet profile is tempered by the strong evaporation. Only at Sacramento and Phoenix is the daily amplitude significantly larger than at other locations. In the first location the cool Pacific air that covers the local area at night reduces all temperatures; in the second the strong nightly radiation losses and continued evaporation during the night combine to chill the surface.

The detailed diurnal course of the energy balance partition is illustrated in three cases in Figs.3, 4, and 5. Fig.3 shows that at Binghamton, N.Y. the maximum potential evaporation rate is about 0.5 mm/h and that during the daytime the air is heated. Heat is also flowing into the soil, but more of it is released during the night in an amount nearly equal to the radiation losses. During the day the air is unstable, and at night an inversion prevails that prevents heat and mass exchange between the surface and the air as shown in Fig.6.

At Phoenix, Arizona (Fig.5) a different situation obtains. The potential evaporation reaches a daily maximum of 0.9 mm/h, and the heat exchange with the air is slightly positive, day and night. The inversion is a permanent feature at all hours, as shown in Fig.6. In contrast to A, the soil heat flux is

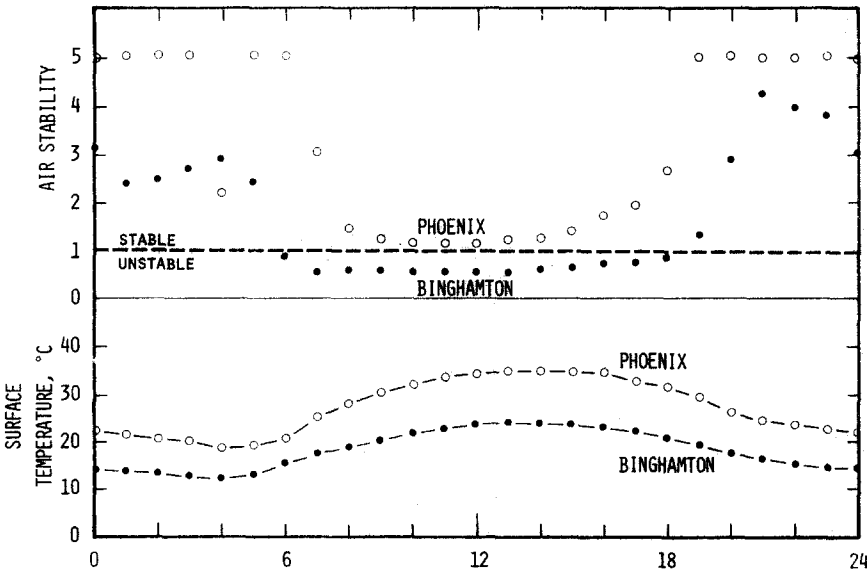


Fig.6. Hourly values of the air stability in the surface boundary layer (top) and of the surface temperature (bottom) during potential evaporation in a temperate and humid summer climate (Binghamton, N.Y.) and in a hot and dry summer climate (Phoenix, Ariz.).

pronounced. Its maximum negative value precedes the radiant energy peak by about 3 h, equal to the value derived from the mathematical theory of heat flow, as shown by Van Wijk and De Vries (1966). Thus, the latent heat losses are below the net radiation in the morning and considerably above it in the late afternoon. Experimentally, this was found by Fritschen and Van Bavel (1962) for the same location.

It is also noteworthy that evaporation continues at night at around 0.05 mm/h according to our model, again in agreement with experimental observations (Van Bavel, 1966). At the two humid area locations, Binghamton and Houston (Figs.3, 4) the losses at night are negligible, and a small amount of condensation is actually predicted, as indicated in the graph.

Fig.6 gives the hourly value of the air stability as defined in eq.7, and the computed surface temperature under conditions of potential evaporation at the two most divergent locations.

At Binghamton the stability factor is less than 1 during the day, causing the vertical transport intensity to almost double over its adiabatic value. At night the reverse takes place. At Phoenix the stability factor remains larger than 1, the midday values being close to the adiabatic value. However, at night the inversion is strong, virtually isolating the surface from the bulk air.

With regard to the surface temperature, the nocturnal minimum occurs in both cases just before sunrise, whereas the maximum at Binghamton is close to true noon, slightly later at Phoenix. These predictions agree qualitatively with oft-reported experimental data.

Comparison with standard combination method

The foregoing estimates of hourly and daily potential evaporation rate from a wet, bare soil were obtained with a complex model of a number of physical processes taking place in the boundary layer — both in the soil and the atmosphere. It is of obvious importance to know whether these estimates are substantially different from those obtainable by simpler methods. For these we have chosen the combination method, using hourly data and summing the hourly evaporation rates, as well as the even simpler method of using daily average data for the 4 required parameters.

The formula used can be given in the following form (see Van Bavel, 1966):

$$E = \frac{s R_n / L + (D_a / R_a)}{s + 1} \quad (\text{kg m}^{-2} \text{ s}^{-1}) \quad (15)$$

in which R_n is the net radiant balance of the surface in W m^{-2} , L the heat of vaporization in J kg^{-1} , D_a the saturation deficit of the air in kg m^{-3} and R_a the aerodynamic “resistance”, defined by eq.9. The number s is dimensionless and depends upon the ambient temperature T_a in $^{\circ}\text{C}$.

A close approximation is obtained from a polynomial fit of the table given in Van Bavel (1966):

$$s = 0.921 - 0.002632 T_a + 0.003075 T_a^2$$

The soil heat flow is neglected, as are deviations from neutrality in the boundary layer. R_a is calculated from eq.9, using $Z_0 = 0.01$ m, as in the complex model.

R_n is found from:

$$R_n = (1 - a) R_g + R_1 - \epsilon \sigma T_a^4 \quad (\text{W m}^{-2})$$

The value used for a was 0.10 and for ϵ it was 0.98. R_1 was obtained as shown in eq.4. Thus, the calculation of R_n was identical to that in the complex model, except that a and ϵ were constant, and that the air temperature was used instead of the actual surface temperature.

The results of this comparison are shown in Table IV. On the whole, the hourly combination method gives somewhat lower values than the simulation

TABLE IV

A comparison of values for the 24-h potential evaporation for 8 different climates computed by the present, comprehensive model, by the combination method using hourly weather parameters, and by the same method using the 24-h average of the same parameters (relative values are given in parenthesis)

	Present model	Hourly combination	Daily combination
Binghamton	4.55	4.15 (.91)	3.97 (.87)
Des Moines	5.35	5.02 (.94)	4.93 (.92)
Houston	6.06	5.42 (.90)	5.23 (.86)
Lubbock	7.69	7.75 (1.01)	7.57 (.99)
Phoenix	8.06	8.62 (1.06)	8.15 (1.01)
Sacramento	7.70	7.20 (.94)	6.67 (.87)
Seattle	4.63	4.18 (.90)	4.01 (.87)
Lubbock extreme	12.07	11.78 (.98)	11.45 (.95)
Average ratio		(.95)	(.92)

model, particularly in the more humid climates. When the calculation is based upon the daily averages the difference is slightly larger. Nevertheless, the differences among the three methods under any of the 8 different weather patterns appear not significant enough to warrant the use of the complex model developed in this report, or, for that matter, to justify using anything but daily averages in eq.15. It is of particular interest that this conclusion is

apparently not affected by the occurrence of strong advective effects.

An experimental study of bare soil evaporation by Van Bavel (1966) led to essentially the same conclusion. Its practical significance is further underscored by the deduction from the present work that the concept of potential evaporation, even from a simple surface, escapes precise definition. Useful as the idea may be, its precision is no more than 5–10% as a quantitative tool. The value of E_p depends upon soil properties and its drainage status, and the differences that are attributable to the variation in non-climatic variables appear as large as those between the three different methods for calculating E_p as shown in Tables III and IV.

Given, in addition, the limited accuracy of available data on global irradiance and windspeed, we conclude that, for general purposes, the combination method as given in eq.15 and based on daily averages, will be sufficient. If, for some reason, the diurnal distribution of E is needed, one must use or generate hourly numbers from the available data and use these in eq.15.

Actual evaporation from a drying soil

We have already shown that our simulation model of the combination model of bare soil evaporation is not limited to the potential evaporation phase. To explore this aspect, 10-day and 20-day runs were made. Details of the results of the 10-day simulation for Lubbock, Texas are given in Table V.

As stated before, during the first 4 days the surface was continuously at a relative humidity of 1.0 and the evaporation proceeded at the potential rate, between 7 and 8 mm per day. A reduction in surface humidity began on the afternoon of the fifth day, and thereafter the water loss declined at an accelerating rate. The results do not suggest clearly distinguishable “weather-limited” and “soil-limited” phases.

Along with the decline in latent heat flux, our results give a decrease in net radiation, a sign reversal of the soil heat, indicating a warming of the soil, and a similar reversal of the heat flux in the air, which rises to large values. The contrast between soil and air heating is remarkable: the former is inhibited by the drying of the surface soil and its decreased heat conductance; the latter is enhanced because of the decreased stability of the air.

The results also show that, as the soil dries, the daytime surface temperature rises steeply, but the nighttime temperature only slightly. Thus, the daily surface amplitude on the 10th day is about double that of the first day.

It is also to be noted that even on the 10th day the evaporation is by no means negligible and, indeed, its magnitude is comparable to the drainage rate. Thus, the soil storage reservoir continues to be depleted, the rate on the 10th day being 1.6% of the total amount of water present. It should be understood that for soil profiles of different properties rather different results will be obtained. For instance, a sandy soil can be expected to show greater initial drainage losses and a more sudden decline in evaporation and

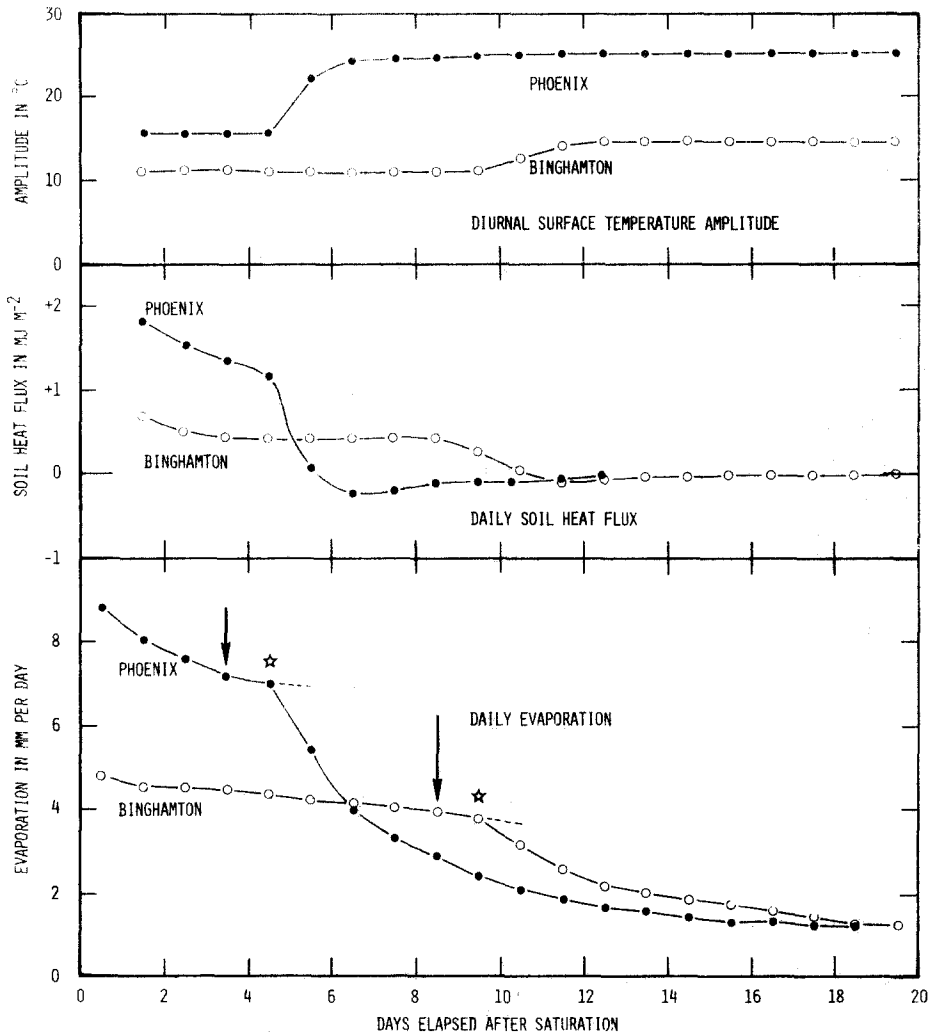


Fig. 7. Daily values of bare-soil evaporation (bottom), of soil heat flux (center) and of the surface-temperature amplitude (top) during a 20-day simulation of the drying of an initially saturated loam profile in a temperate and humid summer climate (Binghamton, N.Y.) and a hot and dry summer climate (Phoenix, Ariz.).

drainage rate. This element of the problem was analyzed by Hillel and Van Bavel (1976).

A further exploration of the predicted evaporation from drying soil was obtained from 2 simulations over 20 days for the two contrasting summer climates of Binghamton, N.Y. and Phoenix, Arizona. Some of the simulation results are given in Fig. 7. In both locations there was a period during which the surface relative humidity remained constant and equal to 1. The last day on which this occurred is indicated by an arrow in Fig. 7. On the following

TABLE V

Water balance (evaporation, E and drainage, D), energy balance (net radiation, R_n , latent heat flux, LE , air heat flux, A , soil heat flux, S), surface properties (max, min, and amplitude of temperature, relative humidity at noon, Rh_s) and boundary layer stability (St), at noon for a drying, initially saturated profile of loam at Lubbock, Texas.

	E	D	R_n	LE	A	S	$T_{s,max}$	$T_{s,min}$	Ampl.	Rh_s	St
	(mm day ⁻¹)			(MJ m ⁻² day ⁻¹)			(°C)				
1	8.02	66.9	17.32	-19.58	0.10	2.15	30.3	18.5	11.8	1.00	.79
2	7.69	15.6	17.53	-18.78	0.20	1.04	30.2	18.1	12.1	1.00	.79
3	7.38	10.2	16.84	-18.02	0.26	0.91	29.9	18.1	11.8	1.00	.81
4	7.02	7.7	15.91	-17.14	0.38	0.84	29.7	18.1	11.6	1.00	.83
5	6.82	6.2	15.51	-16.65	0.42	0.73	29.9	18.2	11.7	1.00	.85
6	5.73	5.0	14.84	-13.99	-0.77	-0.08	34.3	18.3	16.0	.90	.79
7	3.92	4.4	14.12	-9.57	-3.84	-0.70	37.6	18.8	18.8	.54	.55
8	3.15	3.8	13.76	-7.69	-5.53	-0.53	38.2	19.2	19.0	.42	.47
9	2.81	3.3	13.58	-6.86	-6.33	-0.40	38.6	19.5	19.1	.41	.46
10	2.40	2.9	13.40	-5.86	-7.15	-0.39	38.9	19.7	19.2	.31	.47

day, a small depression occurred in the afternoon followed by ever drier surface conditions on succeeding days. It appears that, in spite of the non-constant evaporation rates during the "potential" phase, it is possible to discern two stages of evaporation, with the break between them occurring on the first day that the air at the surface is not at the saturation humidity. This transition is marked in Fig.7 by an asterisk.

In a temperate, humid climate the first stage can last longer than in a hot and arid climate. However, the duration of the first stage would obviously also depend on soil type. The second stage of drying is typified at first by a rapid decline that gradually tapers off. However, no distinct "third stage" of drying is discernible. Toward the end of the simulation period, the daily rate appeared nearly constant, but in fact continued to decline slowly. Experimental data could easily create an impression of a constant "soil controlled" third stage, because of the inevitable measurement errors.

However, an examination of the diurnal rate of evaporation shows a typical energy-regulated variation, in agreement with experimental data reported by Van Bavel and Reginato (1965). Fig.8 shows the calculated diurnal variation in Phoenix on the 20th day of simulation, totalling 1.05 mm.

It is of interest to note that in a dry, hot climate the evaporation rates can be, for a time, less than in a humid, temperate climate, as the comparison of Binghamton and Phoenix in Fig.7 shows. Eventually the rates become essentially equal. But, it appears that the accumulated evaporation loss over time will tend to be larger in the more evaporative environment.

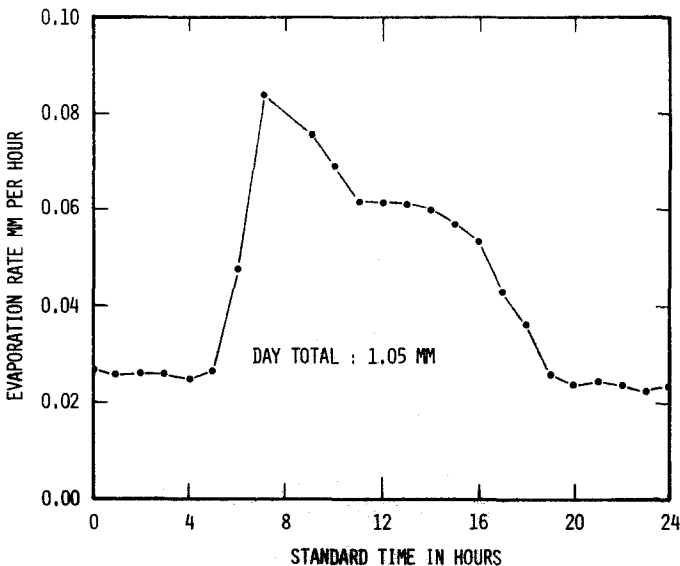


Fig.8. Hourly values of the evaporation from a loam-soil profile on the 20th day of continuous drying in a hot and dry summer climate (Phoenix, Ariz.).

Fig.7 also shows the daily heat flow and the daily surface temperature amplitude. The latter is predicted to be essentially constant during each of the two phases of drying. However, the absolute surface temperature slowly rises as the evaporation declines. Both effects are also evident from Table V.

In general, we can conclude that our model is capable of predicting both potential and less-than-potential rates of evaporation from common weather data, provided the hydraulic and thermal properties of the soil are known. Of these, the hydraulic properties are surely the most important. Staple (1974) has described a model that neglects the flow of heat altogether, and applied it, using daily averages of weather data, with fairly good results.

An important issue is how one may know, in a real situation, whether the transition from the first to the second stage has occurred. Our model suggests, of course, that even a direct measurement of the evaporation rates may not easily give this answer, apart from the daily variability of the weather in a real situation. Increases in albedo may occur well before potential evaporation ceases, and are therefore not an appropriate criterion. However, the results of Fig.7 suggest that the most sensitive and also practical criterion would be the surface-temperature amplitude.

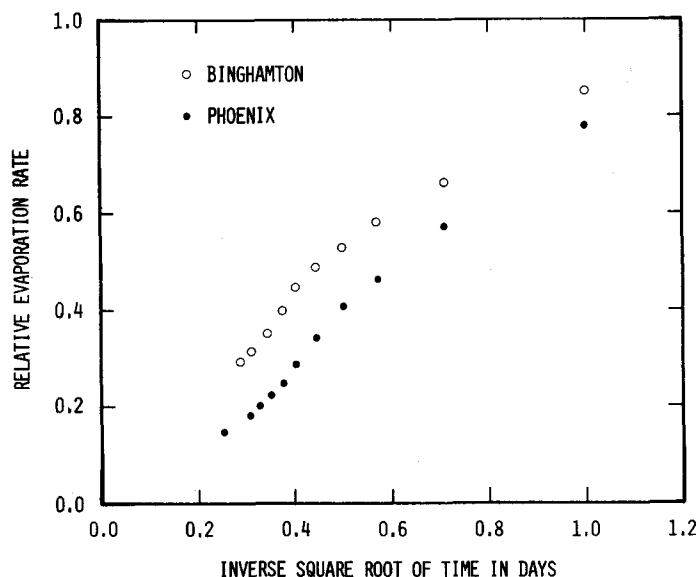


Fig.9. Daily evaporation rate from bare soil during the falling rate stage relative to its value on the day preceding the onset of the falling rate stage (potential evaporation) against the square root of time elapsed in days. The relation is portrayed for a temperate and humid summer climate (Binghamton, N.Y.) and a dry and hot summer climate (Phoenix, Ariz.).

A further question is whether the drying rates during the second phase can be empirically predicted for a given soil by an inverse square-root-of-time relation as suggested by Ritchie (1972). This question is examined in Fig.9, by plotting the value of $1/\sqrt{\text{days}}$, commencing with the first day of

the falling rate stage, identified in Fig.7, with an asterisk, against the relative evaporation rate on succeeding days. The relation is not far from linear for both the Phoenix and Binghamton climate, but the one is distinctly different from the other, though in both cases the soil properties are the same. This finding suggests that empirical relations such as Ritchie's can be used only for a given soil and climate combination.

We must emphasize that all results obtained by our model are theoretical and approximate. The soil is divided into discrete layers and certain conditions are assumed: zero heat flux and unit hydraulic gradient at the bottom, no evaporation other than at the surface, and no water transfer in vapor form. Many other relations are simplified. The main advantage of our approach is that available numerical data on weather and soil properties are readily used, and that their effect can be quickly explored. If necessary, a layered soil situation, as well as rainfall, infiltration and runoff can be added to the model. No analytical methods for the combination of all these elements appear to exist.

SUMMARY AND CONCLUSIONS

A numerical method is formulated whereby the surface-energy balance of a bare soil and the transport of heat and water in both the atmospheric boundary layer and in the soil are combined for calculating the evaporation rate. Thus, it is an extension of the original combination or Penman formula to find the potential evaporation. The present model is much more comprehensive and accounts for soil properties and changes therein as evaporation proceeds. Similarly, it reflects changing surface properties and atmospheric stability. Thus it is a dynamic model, requiring standard weather data and an initial soil condition as the inputs.

The main conclusion is that the historic concept of potential evaporation is imprecise, as the evaporation rate from a wet soil surface can vary by more than 10%, depending on soil properties. If potential evaporation is more narrowly defined as the rate prevailing from a soil that, initially saturated, has drained freely for 24 h, a consistent though still not entirely rigorous concept is obtained.

We show results of a calculation of E_p , so defined, for 8 widely different climatic situations and find that the calculated evaporation rates are not materially different from those obtainable from the simple combination method, even when daily averages of the pertinent weather data are used.

Extension of the calculation of evaporation beyond the potential phase shows that it is clearly distinguishable from a second, so called "falling-rate" stage. This second stage should perhaps more appropriately be identified as the "subpotential" phase. However, a third or constant rate stage apparently cannot be identified. Also, during the first stage the evaporation rates are not constant, but declining even when the weather is constant.

The transition for the first to the second phase of bare-soil drying is not so

much due to changes in albedo, but primarily to the hydraulic properties of the soil and the occurrence of relative humidities at the surface smaller than 1. The transition point is marked by a rapid increase in the surface temperature amplitude.

Prediction of evaporation rates during the second stage from standard weather data requires information on the hydraulic properties of the soil profile and, also, on its thermal properties, though the first are the most important.

REFERENCES

- Conway, J. and Van Bavel, C. H. M., 1967. Evaporation from a wet soil surface calculated from radiometrically determined surface temperatures. *J. Appl. Meteorol.*, 6: 650—655.
- De Vries, D. A., 1966. Thermal properties of soils. In: W. R. van Wijk (Editor), North-Holland, Amsterdam, 2nd ed., pp. 210—235.
- De Wit, C. T. and Van Keulen, H., 1972. *Simulation of Transport Processes in Soils*. Pudoc, Wageningen, 100 pp.
- Fritschen, L. J. and Van Bavel, C. H. M., 1962. Energy balance components of evaporating surfaces in arid lands. *J. Geophys. Res.*, 67: 5179—5185.
- Hillel, D. I., 1971. *Soil and Water*. Academic Press, New York, N.Y., 288 pp.
- Hillel, D. I., 1975. Simulation of evaporation from bare soil under steady and diurnally fluctuating evaporativity. *Soil Sci.*, 120: 230—237.
- Hillel, D. I. and Van Bavel, C. H. M., 1976. Dependence of profile water storage on soil texture and hydraulic properties: A simulation model. *Soil Sci. Soc. Am. J.*, in press.
- Hillel, D. I., Van Bavel, C. H. M. and Talpaz, H., 1975. Dynamic simulation of water storage in fallow soil as affected by mulch of hydrophobic aggregates. *Soil Sci. Soc. Am. Proc.*, 39:826—833.
- Jackson, R. D., Reginato, R. J., Kimball, B. A. and Nakayama, F. S., 1974. Diurnal soil-water evaporation: comparison of measured and calculated soil-water fluxes. *Soil Sci. Soc. Am. Proc.*, 38: 861—866.
- Linacre, E. T., 1969. Net radiation to various surfaces. *J. Appl. Ecol.*, 6: 61—75.
- Monteith, J. L., 1963. Gas exchange in plant communities. In: L. T. Evans (Editor), *Environmental Control of Plant Growth*. Academic Press, New York, N.Y., pp. 95—112.
- Penman, H. L., 1948. Natural evaporation from open water, bare soil and grass. *Proc. R. Soc. Lond.*, A193: 120—145.
- Philip, J. R. and De Vries, D. A., 1957. Moisture movement in porous materials under temperature gradients. *Trans. Am. Geophys. Union*, 38: 222—232.
- Pruitt, W. O., Morgan, D. L. and Lourence, F. J., 1973. Momentum and mass transfers in surface boundary layer. *Q. J. R. Meteorol. Soc.*, 99:370—386
- Ritchie, J. T., 1972. Model for predicting evaporation from a row crop with incomplete cover. *Water Resour. Res.*, 8: 1204—1213.
- Sellers, W. D., 1965. *Physical Climatology*. Univ. of Chicago Press, Chicago, Calif.
- Staple, W. J., 1974. Modified Penman equation to provide the upper boundary conditions in computing evaporation from soil. *Soil Sci. Soc. Am. Proc.*, 38: 837—839.
- Szeicz, G., Van Bavel, C. H. M. and Takami, S., 1973. Stomatal factor in the water use and dry matter production by sorghum. *Agric. Meteorol.*, 12: 361—389.
- Van Bavel, C. H. M., 1966. Potential evaporation: the combination concept and its experimental verification. *Water Resour. Res.*, 2: 455—467.
- Van Bavel, C. H. M. and Hillel, D. I., 1975. A simulation study of soil heat and moisture dynamics as affected by a dry mulch. *Proc. Summer Computer Simulation Conf.*, 1975, pp. 815—821.

- Van Bavel, C. H. M. and Reginato, R. J. 1965. Precision lysimetry for direct measurement of evaporative flux. Proc. Int. Symp. Methodol. Plant Eco-Physiol., Montpellier. UNESCO, Arid Zone Res., 25: 129-135.
- Van Bavel, C. H. M., Ahmed, J., Bhuiyan, S. I., Hiler, E. A. and Smajstrla, A. G., 1973. Dynamic simulation of automated subsurface irrigation systems. Trans. Am. Soc. Agric. Eng., 16: 1075-1099.
- Van Keulen, H., 1975. Simulation of water use and herbage growth in arid regions. Pudoc, Wageningen, 176 pp.
- Van Wijk, W. R. and De Vries, D. A., 1966. Periodic temperature variations in a homogeneous soil. In: W. R. van Wijk (Editor), Physics of Plant Environment. North-Holland, Amsterdam, 2nd ed., pp. 102-143.
- Wierenga, P. J. and De Wit, C. T., 1970. Simulation of heat transfer in soils. Soil Sci. Soc. Am. Proc., 34: 845-847.